


ARTICLE **OPEN**


The optimized core peptide derived from CABIN1 efficiently inhibits calcineurin-mediated T-cell activation

 Sangho Lee^{1,2}, Han-Teo Lee², Young Ah Kim², Il-Hwan Lee³, Seong-Jun Kang³, Kyeongpyo Sim³, Chung-Gyu Park^{3,4},
 Kyungho Choi³ and Hong-Duk Youn^{1,2,3} 

© The Author(s) 2022

The C-terminal fragment of CABIN1 interacts with calcineurin and represses the transcriptional activity of the nuclear factor of activated T cells (NFAT). However, the specific sequences and mechanisms through which it binds to calcineurin are unclear. This study determined that decameric peptide (CABIN1 residues 2146–2155) is minimally required for binding to calcineurin. This peptide contains a unique “PPTP” C-terminal sequence and a “PxIxIT” N-terminal motif. Furthermore, p38MAPK phosphorylated the threonine residue of the “PPTP” sequence under physiological conditions, dramatically enhancing the peptide’s binding affinity to calcineurin. Therefore, the CABIN1 peptide inhibited the calcineurin-NFAT pathway and the activation of T cells more efficiently than the VIVIT peptide without affecting calcineurin’s phosphatase activity. The CABIN1 peptide could thus be a more potent calcineurin inhibitor and provide therapeutic opportunities for various diseases caused by the calcineurin-NFAT pathway.

Experimental & Molecular Medicine (2022) 54:613–625; <https://doi.org/10.1038/s12276-022-00772-6>

INTRODUCTION

Calcineurin is calcium and calmodulin-dependent serine/threonine phosphatase that plays a pivotal role in diverse organs or cells, such as the brain, cardiovascular and skeletal muscle, pancreatic β cells, and T lymphocytes^{1–4}. Over the past few decades, many substrates and inhibitors of calcineurin containing conserved motifs for interaction with calcineurin, “PxIxIT” and/or “LxVP,” have been identified. For instance, nuclear factor of activated T cells (NFAT) family members are known calcineurin substrates containing both binding motifs⁵. In calcineurin-regulated NFATs (all NFAT family members except NFAT5), calcineurin dephosphorylates at least 13 conserved phosphorylation sites⁶. These sites are in the NFAT-homology region between the “PxIxIT” and “LxVP” motifs⁷. Several kinases, such as GSK3, CK1, p38, and JNK, phosphorylate these sites. These molecules cause conformational changes, expose nuclear export signals, and mask nuclear localization signals⁸.

Productive activation of T lymphocytes requires T-cell receptor (TCR) signaling and costimulatory signaling to act together. TCR signaling or costimulatory signaling alone leads to T-cell anergy or tolerance^{9,10}. TCR stimulation activates the calcineurin-NFAT pathway by elevating intracellular Ca^{2+} concentrations¹¹, and simultaneous stimulation of TCR/CD28 activates the PKC-MAPK and PKC-IKK-NF κ B pathways^{12,13}. The calcineurin-NFAT and PKC-MAPK pathways activate NFAT and AP-1 (Fos/Jun), which cooperate in the transcriptional activation of proinflammatory cytokines, such as interleukin (IL)-2, IL-3, IL-4, GM-CSF, and IFN- γ , thereby activating T lymphocytes¹⁴. However, PKC activation antagonizes the Ca^{2+} -induced calcineurin-NFAT pathway, despite

being important for T lymphocyte activation¹⁵. PKC-activated p38 phosphorylates nuclear NFATC2 (also known as NFAT1 or NFATp), thereby inducing the export of NFATC2 to the cytosol¹⁶.

The conventional calcineurin inhibitors FK506 and cyclosporin A have serious side effects. However, they are still widely used in autoimmune diseases and organ transplant patients due to their convenient dosing and effectiveness¹⁷. Although several alternative calcineurin inhibitors have been developed over the past few decades, none have become clinical treatments thus far. The VIVIT peptide, an optimized peptide derived from the conserved “PxIxIT” sequence of the NFAT family, blocks the interaction between calcineurin and NFAT without affecting calcineurin phosphatase activity¹⁸. Although this peptide showed potential as an alternative calcineurin inhibitor for various calcineurin-NFAT pathway-dependent diseases, it has a high IC_{50} value and drug delivery limitations¹⁹.

CABIN1 was first identified as an endogenous calcineurin inhibitor protein. Upon T-cell activation, the CABIN1 C-terminal fragment binds to and inhibits calcineurin, thereby blocking NFAT dephosphorylation and repressing *IL-2* promoter transcriptional activation²⁰. Developing alternative calcineurin inhibitors using CABIN1 requires identifying the specific regions that interact with calcineurin. Although the C-terminus of CABIN1 contains a “PxIxIT” motif¹⁹, it is unknown whether this fragment’s calcineurin inhibitory effect is due to the “PxIxIT” motif. In this study, we inhibited the calcineurin-NFAT pathway using a short peptide from CABIN1. We identified the 10 amino acids required for interaction with calcineurin in the CABIN1 C-terminal fragment. This peptide inhibited the calcineurin-NFAT pathway more

¹National Creative Research Center for Epigenome Reprogramming Network, Department of Biomedical Sciences, Ischemic/Hypoxic Disease Institute, Seoul National University College of Medicine, Seoul 03080, Republic of Korea. ²Department of Molecular Medicine & Biopharmaceutical Sciences, Graduate School of Convergence Science, Seoul National University, Seoul 03080, Republic of Korea. ³Department of Biomedical Science, Seoul National University College of Medicine, Seoul 03080, Republic of Korea. ⁴Department of Microbiology and Immunology, Seoul National University College of Medicine, Seoul 03080, Republic of Korea. ✉email: hdyoun@snu.ac.kr

Received: 19 October 2021 Revised: 11 January 2022 Accepted: 15 February 2022
 Published online: 12 May 2022

efficiently than did the VIVIT peptide, without affecting calcineurin phosphatase activity. We demonstrated that these results were due to the “PPTP” sequence following the “PxIxIT” motif. The binding affinity of the CABIN1 peptide to calcineurin depends on the phosphorylation of its ninth threonine residue (residue 2154 in endogenous CABIN1). Furthermore, p38MAPK is a putative upstream kinase of the CABIN1 peptide. Since the optimized CABIN1 peptide harbors an additional “PPTP” sequence, which is phosphorylated under physiological conditions, we suggest that the CABIN1 peptide could be a potent inhibitor of the calcineurin-NFAT pathway *in vivo*.

MATERIALS AND METHODS

Cell culture and transfection

We purchased HEK293T and Jurkat T (E6-1) cells from ATCC (Manassas, VA, USA). We cultured HEK293T cells in Dulbecco's modified Eagle's medium supplemented with 10% (v/v) fetal bovine serum (Gibco, Grand Island, NY, USA) and antibiotics at 37 °C and 5% CO₂ and transfected them using polyethyleneimine (Polysciences, Warrington, FL, USA). We cultured Jurkat T cells in RPMI 1640 medium supplemented with 10% (v/v) fetal bovine serum (Gibco), 2 mM L-glutamine (Gibco), and antibiotics at 37 °C and 5% CO₂. Following the manufacturer's instructions, we transfected Jurkat T cells by electroporation using a Neon™ Transfection System (Thermo Fisher Scientific, Waltham, MA, USA).

Plasmid DNA constructs

This study used the previously described calcineurin catalytic subunit (CNA) isoforms, CABIN1-14, CABIN1-15, tNFATC2, pG5-luc, and NFAT-luc²⁰. We cloned the CNA isoforms into expression vectors such as pVP16, pRSET-A/B, and pCAG-Flag. We obtained oligonucleotides of CABIN1, VIVIT, and chimeric and substituted peptides from Macrogen (Seoul, Korea) or Cosmogentech (Seoul, Korea), and annealed them for hybridization, and inserted them into expression vectors such as pM, pGEX4T-1, pCAG-HA-GST, and pCAG-HA-mCherry. We constructed the pCAG-EGFP-tNFATC2-IRES-mCherry-peptide by replacing the puromycin resistance gene following the IRES segment with the mCherry-tagged peptide. We confirmed all the constructs by sequencing.

Reagents and antibodies

We purchased the anti-GAL4 DNA binding domain (GAL4 DBD) (RK5C1) antibody from Santa Cruz Biotechnology (Dallas, TX, USA) and anti-NFATC2, pan-CNA, and phospho-MAPK Substrates Motif [PXpTP] antibodies from Cell Signaling (Danvers, MA, USA). We purchased anti-β-actin (AC-15) and Flag (M2) antibodies and Anti-FLAG® M2 Affinity Gel from Sigma-Aldrich (St. Louis, MO, USA). We obtained the anti-HA (16B12) antibody from BioLegend (San Diego, CA, USA) and Pierce™ Anti-HA Agarose from Thermo Fisher Scientific. We acquired phorbol myristate acetate (PMA) and ionomycin from Sigma-Aldrich, FK506 from InvivoGen (San Diego, CA, USA), and EO 1428 and TAK 715 from Tocris (Bristol, UK).

Peptide synthesis

Pepton (Daejeon, Korea) synthesized the unlabeled peptides (CABIN1-L-1 [MAGFPPEITVTPPTP] and VIVIT 15-mer [MAGPHPVIVITGPHEE]). GenScript (Piscataway, NJ, USA) synthesized the biotin-labeled peptides (VEET [Biotin-AAAMAGPPHIVEETGPHVI], VIVIT 15-mer [Biotin-AAAMAGPHPVIVITGPHEE], CABIN1-L-1 [Biotin-AAAMAGFPPEITVTPPTP], and phosphorylated CABIN1-L-1 [Biotin-AAAMAGFPPEITVTPP{pTHR}P]). All the peptides were purified by HPLC and were >95% pure, and their molecular weight and composition were analyzed by mass spectrometry.

Luciferase reporter assay

To measure the transcriptional activity of NFAT, we cotransfected Jurkat T cells with GST-tagged peptides and NFAT-luc by electroporation. After 24 h, we pretreated the cells with 0.5 μM FK506 for 1 h and then treated them with 40 nM PMA and 1 μM ionomycin for 8 h. For the mammalian two-hybrid assay, we cotransfected HEK293T cells with GAL4 DBD-tagged CABIN1, VIVIT, chimeric and substituted peptides, VP16 activation domain-tagged CNAβ₂, and pG5-luc (luciferase reporter plasmid containing the GAL4-responsive promoter) for 24 h. We lysed the harvested cells with a luciferase assay lysis buffer (17 mM KH₂PO₄, 183 mM K₂HPO₄, pH 7.8, 0.2%

[v/v] Triton X-100) and sonicated them briefly. We measured luciferase activity for each cell lysate using an Infinite M200 (Tecan, Männedorf, Switzerland). In addition, we confirmed the expression level of the transfected proteins by Western blotting.

Immunoprecipitation assay

We lysed the cells in IP150 buffer and immunoprecipitated Flag- and HA-tagged proteins with Anti-FLAG® M2 Affinity Gel (Sigma-Aldrich) and Pierce™ Anti-HA Agarose (Thermo Fisher Scientific), respectively. The composition of the buffer and the subsequent process was described previously²¹. To quantify the western blot results, we measured the band areas using ImageJ (<https://imagej.nih.gov/ij/>).

Protein purification and in vitro binding assay

GST-tagged peptides and His-tagged CNAα and β₂ were expressed in *Escherichia coli* BL21(DE3)pLysS. When the OD₆₀₀ reached 0.5, we treated the bacteria with IPTG (0.1 mM overnight at 18 °C or 1 mM for 4 h at 37 °C). We purified the proteins as described previously²². We performed a His-pulldown assay with 0.5 ml of IP150 buffer with 0.5 mM EDTA. We mixed His-tagged CNA with GST-tagged peptides and captured it on Ni-NTA agarose beads (Qiagen, Hilden, Germany). We washed the beads three times with binding buffer and analyzed the proteins by western blotting. We pulled down the GST-tagged peptides using Glutathione Sepharose™ 4 Fast Flow (Cytiva, Marlborough, MA, USA) and the biotin-labeled peptides using Streptavidin Agarose Resin (Thermo Fisher Scientific).

In vitro kinase assay

We used the purified GST-tagged peptides for the in vitro kinase assays with activated recombinant kinases obtained from ProQinase GmbH (Freiburg, Germany). We performed the kinase assays in reaction buffer (50 mM HEPES-NaOH, pH 7.5, 3 mM MgCl₂, 3 mM MnCl₂, 3 μM sodium orthovanadate, 1 mM dithiothreitol, 50 μM unlabeled ATP, 5 μCi ³²P-γ-ATP) for 1 h at 30 °C. We stopped the reaction by adding 5× sample buffer and separated the proteins using SDS-PAGE. The gel was stained with Coomassie Brilliant Blue, dried, and developed on X-ray film.

Confocal microscopy and analysis

We transfected Jurkat T cells with the pCAG-EGFP-tNFATC2-IRES-mCherry-peptide by electroporation. After two days, we pretreated these cells with 0.5 μM FK506 for 30 min. Then, we treated them with 40 nM PMA and 1 μM ionomycin under culture conditions for 4 h. Before imaging by a confocal laser scanning microscope (Nikon, Tokyo, Japan), we treated the cells with 10 μg/ml Hoechst 33342 (Invitrogen, Waltham, MA, USA) to stain nuclei. Colocalization analysis of mCherry and Hoechst was performed with ImageJ and its plugin JACoP to measure the Manders coefficient^{23,24}.

Calcineurin activity assay

We measured calcineurin phosphatase activity *in vitro* using a calcineurin phosphatase assay kit (BML-AK804, Enzo Life Sciences, Farmingdale, NY, USA). We incubated GST or GST-tagged peptides with CNA for 30 min at room temperature and then followed the manufacturer's instructions. To measure endogenous calcineurin phosphatase activity, we transiently transfected Jurkat T cells with CAG-HA-mCherry-peptides by electroporation. After 24 h, we pretreated the Jurkat T cells with FK506 for 1 h before activating them with PMA and ionomycin. Next, we washed the cells with TBS buffer (20 mM Tris, pH 7.2, 150 mM NaCl), resuspended them with lysis buffer from the calcineurin cellular activity assay kit (BML-AK816, Enzo Life Sciences), and kept them on ice for 30 min. We collected the lysate supernatant and removed free phosphate by gel filtration using the Desalting Column Resin included in the kit. Next, we followed the manufacturer's instructions.

Real-time quantitative PCR

We collected Jurkat T cells with QIAzol Lysis Reagent (Qiagen) to extract total RNA. We reverse transcribed cDNAs from isolated RNA using AMV Reverse Transcriptase and random hexamers. We performed real-time quantitative PCR for each cDNA using TB Green® Premix Ex Taq™ (TaKaRa, Kusatsu, Japan) on a CFX Connect Real-time PCR Detection System (Bio-Rad, Hercules, CA, USA) and normalized the expression to that of *18S rRNA* or *GAPDH*. Supplementary Table 1 describes the primers used.

mRNA sequencing and analysis

We pretreated Jurkat T cells expressing HA-mCherry-tagged peptides with FK506 for 1 h before activating them with PMA and ionomycin for 8 h. We then extracted RNA from these cells. Construction of the cDNA library and next-generation sequencing was performed at LAS (Gimpo, Korea). We sequenced all samples on an Illumina NextSeq 500 system with 75 paired-end reads. For the RNA sequencing analysis, reads for each sample were aligned to the human genome (GRCh37/hg19 genome assembly) using STAR 2.4.0.1²⁵ with default settings. We used HOMER tools to quantify and normalize the defined genes in RefSeq transcripts. FPKM normalized genes were hierarchically clustered using Cluster3.0²⁶. We visualized refined data with Java Treeview (<http://jtreeview.sourceforge.net>). We conducted gene ontology analysis of each cluster using the DAVID web tool (<https://david.ncicrf.gov>). Finally, we visualized the expression levels of target genes using the Integrative Genomics Viewer (<http://software.broadinstitute.org/software/igv>). The raw data were submitted to the NCBI Gene Expression Omnibus under accession number GSE185561.

Flow cytometry

We quantified the expression of mCherry-tagged VIVIT peptides using LSRII (SORP) (Becton Dickinson, Franklin Lakes, NJ, USA). We analyzed the results with FlowJo (Tree Star, Inc., Ashland, OR, USA).

Mass spectrometry

We purified HA-mCherry-tagged CABIN1-L-1-2 peptides expressed in Jurkat T cells by immunoprecipitating 4 mg of lysates with Pierce™ Anti-HA Agarose. We eluted the bead-bound proteins by competition with 1 mg/ml HA peptide. After separation by SDS-PAGE and staining with Coomassie Brilliant Blue, we analyzed the purified proteins by LC-MS/MS (ProteomeTech, Inc., Seoul, Korea).

Surface plasmon resonance

Using a Biacore T200 (Cytiva), we captured the biotin-labeled peptides on the surface of a Series S Sensor Chip SA (Cytiva). We serially diluted purified His-tagged CNA in HBS-EP + (10 mM HEPES, pH 7.4, 0.15 M NaCl, 3 mM EDTA, 0.05% surfactant P20) and passed it sequentially over three flow cells (flow cell 1: biotin-VEET, flow cell 2: biotin-CABIN1-L-1, flow cell 3: biotin-p-CABIN1-L-1). Each cycle was performed at 25 °C at a flow rate of 30 µl/min with 120 s of contact and 240 s of dissociation. We analyzed the kinetics of interactions using BIAevaluation 3.2 RC1 (Cytiva).

Statistics

All data are presented as the mean ± standard deviation from at least three biologically independent trials. We calculated *p*-values using a two-tailed Student's *t*-test to compare two groups and using a two-tailed one-way ANOVA with Tukey's multiple comparison test to analyze multiple groups. The *p*-values <0.05, <0.01, and <0.001 appear as single, double, and triple asterisks, respectively. NS indicates a nonsignificant difference (*p* ≥ 0.05).

RESULTS

The 10 amino acids of CABIN1(2146–2155) are essential for the interaction with calcineurin

To determine the minimal sequence binding to calcineurin, we separated the first 13-amino acid segment containing the “PxlIT” motif (named CABIN1-L) from CABIN1-14 (Fig. 1a). We performed a mammalian two-hybrid assay using the GAL4 DBD-tagged CABIN1 peptides and VP16 activation domain-tagged CNA (Fig. 1b, c, Supplementary Fig. 1a, b). Our results confirmed that CABIN1-14 binds to CNA, as previously reported²⁰, while the other sequences (CABIN1-15) did not.

We designed several peptides by sequentially removing the CABIN1-L C-terminal amino acid residues (Fig. 1a; CABIN1-S–CABIN1-L). The mammalian two-hybrid interaction assay showed that CABIN1-L and CABIN1-L-1 had a significantly stronger affinity for CNA than CABIN1-14. However, CABIN1-L-2 completely lost its binding affinity to CNA despite its higher expression level (Fig. 1b). Next, we designed additional peptides by sequentially removing the CABIN1-L-1 N-terminal amino acid residues (Fig. 1a; CABIN1-L-1-1–CABIN1-L-1-4). CABIN1-L-1-1 and CABIN1-L-1-2 still bound to CNA, but CABIN1-L-1-3 lost its binding affinity (Fig. 1c).

The immunoprecipitation assays using the GAL4 DBD-tagged CABIN1 peptide and Flag-tagged CNA showed identical results (Supplementary Fig. 1d, e). These results demonstrate that the 10 amino acids from proline 2146 to proline 2155 of full-length CABIN1 form the minimal sequence needed for interaction with calcineurin.

The PPTP sequence following the “PxlIT” motif is critical for the interaction with calcineurin

Previous research demonstrated the biochemical and structural importance of the “PxlIT” motif^{18,27}, but the role of the neighboring sequences around the “PxlIT” motif in calcineurin binding remains unclear. Since proline 2155 does not belong to the “PxlIT” motif, we needed to clarify the role of the C-terminal “PPTP” sequence following the “PxlIT” motif. To compare the CABIN1 and VIVIT peptides under the same conditions, we used the VIVIT decamer (VIVIT 10-mer) as a control. We constructed a chimeric peptide by swapping the C-terminal sequences of the VIVIT and CABIN1 peptides and conducted a mammalian two-hybrid assay (Fig. 1d, Supplementary Fig. 1c). The C-terminal “PPTP” sequence enhanced the interaction with CNA by 4.76-fold (VIVIT PPTP vs. VIVIT 10-mer), while the N-terminal “PVIVIT” enhanced it by 1.93-fold (VIVIT PPTP vs. L-1-2 WT). This result suggests that the C-terminal “PPTP” sequence also plays an important role in the interaction with calcineurin.

Next, we investigated whether the N-terminal sequence in front of “PxlIT” (“AGPH” in the VIVIT peptide and “FP” in CABIN1-L-1) contributed to the interaction with calcineurin. Adding “AG,” “PH,” or “FP” before the “PxlIT” motif did not affect the interaction with calcineurin (Supplementary Fig. 2a, b). In addition, these sequences did not affect the inhibitory effect of the calcineurin-NFAT pathway (Supplementary Fig. 2c). In the case of the VIVIT peptide, the C-terminal glutamate repeats decreased protein stability (Supplementary Fig. 3a–d).

The CABIN1 peptide is a stronger calcineurin-NFAT pathway inhibitor than the VIVIT peptide

To investigate the inhibitory effect of the CABIN1 peptide on the calcineurin-NFAT pathway, we cotransfected the GST-tagged CABIN1-L-1-2 or VIVIT peptide into Jurkat T cells with a luciferase reporter gene under the control of three repeated NFAT binding sites. Upon treatment with PMA and ionomycin, expression of the GST-tagged CABIN1-L-1-2 or VIVIT peptide repressed luciferase activity compared with the negative control. The inhibitory effect of CABIN1-L-1-2 was approximately four times stronger than that of the VIVIT peptide (Fig. 2a). To confirm that this result is due to NFATC2 dephosphorylation by calcineurin, we performed an NFAT mobility shifting assay. In T cells, NFATC1 and NFATC2 are hyperphosphorylated, and calcineurin dephosphorylates them in response to calcium signaling⁸. Hyperphosphorylated NFATs are localized in the cytosol, whereas dephosphorylated proteins are localized in the nucleus and migrate faster in gels than hyperphosphorylated proteins²⁸. Similar to FK506, the CABIN1 peptide significantly inhibited the NFATC2 band shift upon treatment with PMA and ionomycin (Fig. 2b). The VIVIT peptide also reduced the dephosphorylation of NFATC2, but its inhibitory effect was weaker than that of the CABIN1 peptide (Fig. 2b, c).

Next, we constructed plasmids expressing EGFP-tagged truncated NFATC2 (tNFATC2; 2–460 amino acids) and mCherry-tagged each peptide to confirm the contribution of these peptides to NFAT nuclear import. The proportion of nuclear-localized tNFATC2 was lowest in the FK506-treated cells and slightly higher in the Jurkat T cells coexpressing the CABIN1-L-1-2 peptide. Moreover, the Jurkat T cells coexpressing the VIVIT peptide showed a significantly higher proportion of nuclear-localized tNFATC2 than the cells coexpressing the CABIN1-L-1-2 peptide (Fig. 2d, e). Altogether, these results demonstrate that the CABIN1 peptide

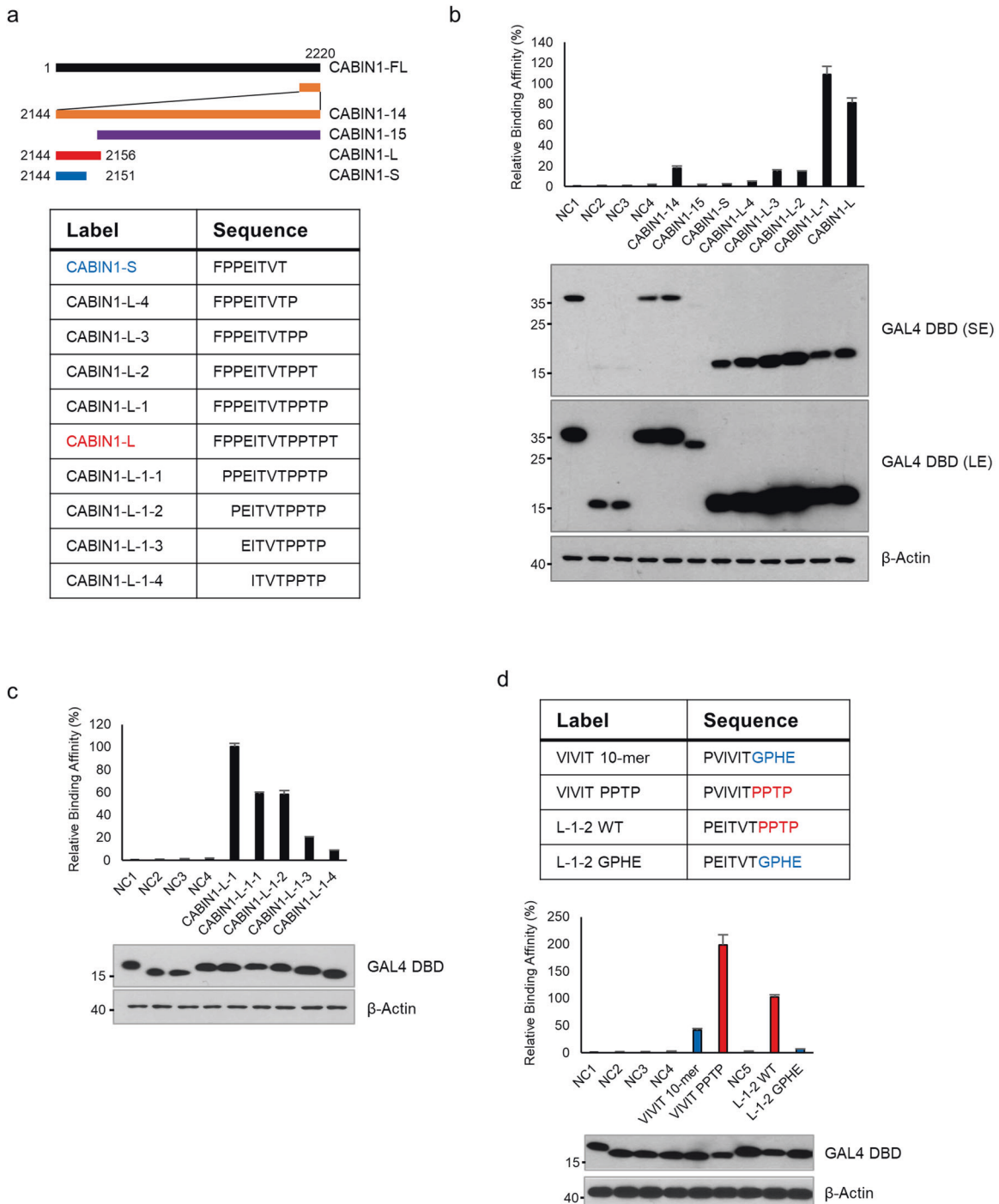


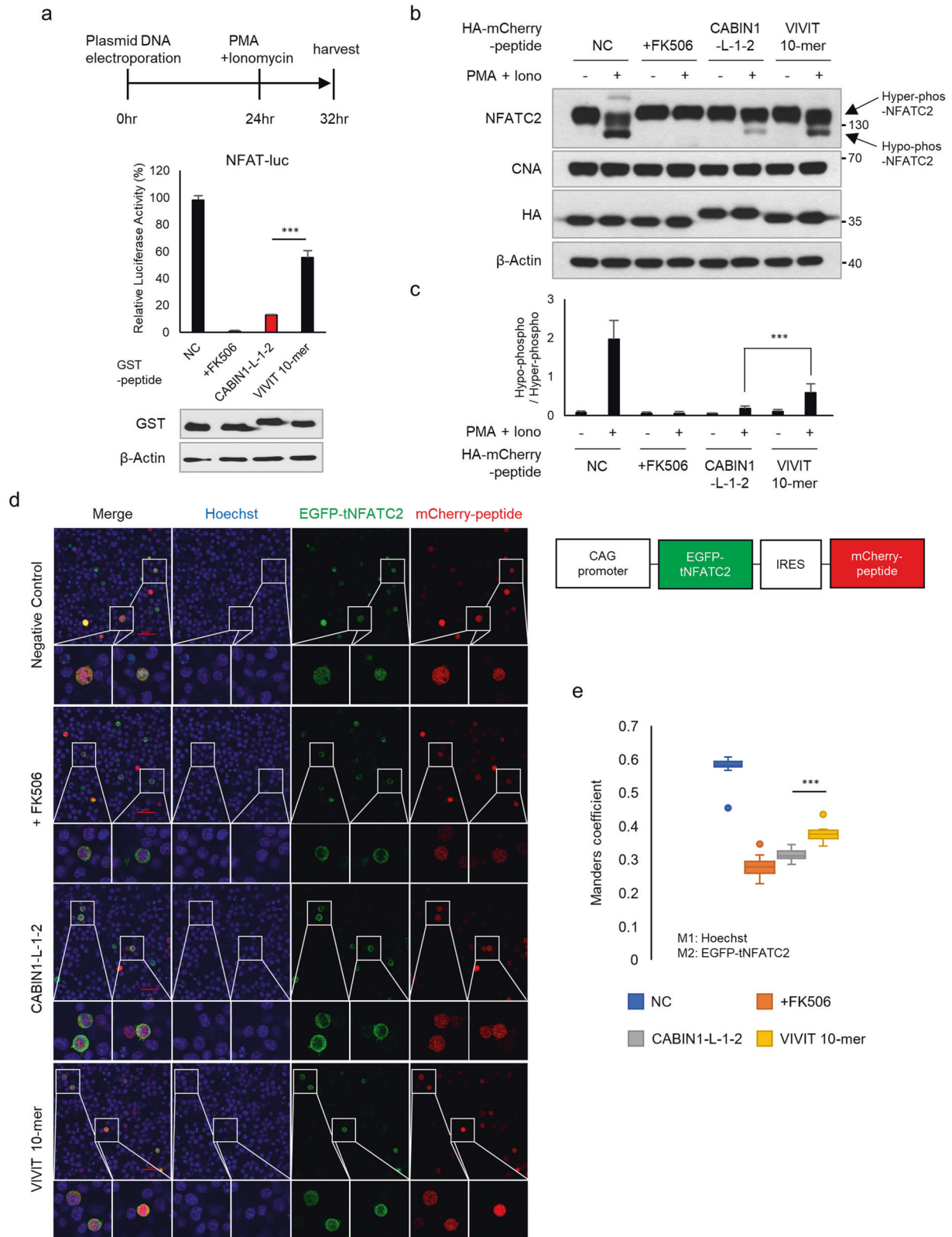
Fig. 1 The short peptide from the CABIN1 C-terminus is essential for interaction with calcineurin. **a** Schematic diagram and sequence of CABIN1 fragments. **b, c** A mammalian two-hybrid assay was performed using VP16 AD-CNA β_2 and GAL4 DBD-CABIN1 peptides (**b** CABIN1-14, -15, -S ~ L; **c** CABIN1-L-1 ~ L-1-4) in HEK293T cells. **d** Sequences of CABIN1-L-1-2, the VIVIT 10-mer and the chimeric peptide (top). A mammalian two-hybrid assay using these peptides was performed (bottom). The compositions of the transfected DNA are described in Supplementary Fig. 1a–c. All experiments were repeated three times and are presented as the mean \pm standard deviation. The expression levels of the peptides were confirmed by western blotting. SE short exposure, LE long exposure, NC negative control, WT wild-type.

blocks the dephosphorylation and nuclear translocation of NFATC2 more efficiently than the VIVIT peptide does.

The CABIN1 peptide blocks T lymphocyte activation

To confirm whether the CABIN1 peptide blocks T lymphocyte activation by interfering with the calcineurin-NFAT interaction, we sequenced the RNA of Jurkat T-cell lines stably expressing the negative control (mCherry only) and mCherry-tagged CABIN1

peptide. We found 685 genes affected by PMA and ionomycin treatment in the negative control cells (Fig. 3a, Supplementary Table 2). We focused on cluster III of the four clusters, which contained genes with increased expression levels in the negative control group upon treatment with PMA and ionomycin and reduced expression levels in the CABIN1-expressing cells and the FK506-treated cells (Supplementary Table 3). Gene Ontology analysis revealed that the genes in cluster III are related to



chemokines, cytokine signaling, and the immune response (Fig. 3b). Furthermore, upon T-cell activation, the CABIN1 peptide, and FK506 reduced the RNA levels of representative T-cell activation markers, including *IL2*, *IL3*, *NFATC1*, and various chemokine ligands (*CCL4*, *CCL20*, and *CXCL8*). In addition, the

CABIN1 peptide and FK506 repressed *CD27* and *CD70*, which regulate the T-cell costimulatory pathway (Fig. 3c). Real-time quantitative PCR analysis of these genes showed that the CABIN1 peptide reduced the RNA levels of these genes more efficiently than the VIVIT peptide (Fig. 3d).

Fig. 2 The CABIN1 peptide inhibits the CN-NFAT pathway more efficiently than the VIVIT peptide. **a** A luciferase reporter assay was performed to measure NFAT transcriptional activity. Jurkat T cells expressing GST-tagged peptides were treated with PMA and ionomycin for activation. Jurkat T cells expressing only GST were used as a negative control, and cells treated with 0.5 μ M FK506 were used as a positive control ($n = 3$). **b** NFAT mobility shifting assays were performed using Jurkat T cells expressing HA-mCherry-tagged peptides. For dephosphorylation of NFATC2, Jurkat T cells were treated with PMA and ionomycin for 2 h. **c** Hyper- and hypophosphorylated NFATC2 of **b** was measured using ImageJ, and the hypo/hyper ratio was calculated ($n = 7$). **d** Snapshot images of the activated Jurkat T cells expressing the indicated peptides and tNFATC2 were obtained using confocal microscopy. The expression and localization of peptides and tNFATC2 are shown as mCherry (red) and EGFP (green), respectively. Nuclei were stained with Hoechst (blue). Scale bar, 50 μ m **e** Nuclear-localized tNFATC2 was measured by calculating the colocalization ratio between Hoechst (M1) and EGFP (M2). (NC and FK506, $n = 10$; CABIN1-L-1-2 and VIVIT 10-mer, $n = 12$) Data are representative of independently repeated experiments and presented as the mean \pm standard deviation. Statistical differences were determined using a two-tailed Student's *t*-test (**a**, **c**) or one-way ANOVA (**e**). *** $p < 0.001$, NC negative control.

The CABIN1 peptide does not inhibit calcineurin phosphatase activity

The VIVIT peptide binds to distinct regions of the CNA catalytic site and disrupts the CNA-NFAT interaction²⁷. To confirm that the CABIN1 and VIVIT peptides have the same mechanism of action, we conducted a peptide competition assay. The CABIN1 peptide dose-dependently interfered with the interaction between the GST-tagged VIVIT peptide and His₆-tagged CNA and vice versa (Fig. 4a). In addition, ionomycin treatment did not affect the interaction between CNA and the CABIN1 or VIVIT peptide (Fig. 4b). This result confirms that the CABIN1 peptide, VIVIT peptide, and fused tag (GAL4 DBD) do not interfere with the active site of CNA because CNA's autoinhibitory domain blocks the active site in the steady-state and releases it through a calcium-induced conformational change upon ionomycin treatment⁵. Next, we measured calcineurin phosphatase activity in Jurkat T cells expressing each peptide or treated with FK506 (Fig. 4c). FK506, which interferes with the active site of CNA, decreased the phosphatase activity of CNA, but the CABIN1 and VIVIT peptides did not. These peptides also did not reduce the phosphatase activity of CNA in vitro (Fig. 4d).

The C-terminal PPTP sequence is important for interaction with calcineurin

To understand how the "PPTP" sequence contributes to the binding affinity to CNA, we compared the binding affinity of each GST-tagged peptide for CNA at the cellular level and in vitro (Fig. 5a). The "PPTP" sequence enhanced CNA binding affinity only at the cellular level, not in vitro, suggesting that this effect was due to post-translational modifications (PTMs) on residues of "PPTP." Next, we substituted one or all of the PPTP residues with amino acids corresponding to each residue of the GPHE sequence of the VIVIT peptide. We conducted a mammalian two-hybrid assay using these constructs and CNA to determine which modification affected the affinity (Fig. 5b). As a result, all the substitutions dramatically disrupted the interaction with CNA, implying that every residue in the "PPTP" sequence is crucial for the interaction with CNA. This result suggests that the "PPTP" sequence could be a substrate motif of an upstream enzyme capable of modifying residues. Subsequent experiments using these substitutions revealed that threonine 9 and proline 10 of the CABIN1 peptide might be targets of PTM because, in vitro, peptides with substitutions at these residues exhibited binding affinities for CNA comparable to that of wild-type CABIN1, while in cellular experiments, all the substitutions disrupted the interaction with calcineurin (Fig. 5c).

Phosphorylation of CABIN1 T2154 is critical for the interaction with calcineurin

We investigated the phosphorylation and *O*-linked glycosylation of threonine residues and hydroxylation of proline residues of the peptides containing "PPTP". First, we investigated whether proline residues of "PPTP" were hydroxylated. We treated Jurkat T cells expressing the mCherry-tagged CABIN1 peptide with dimethylallylglycine (DMOG), a prolyl hydroxylase inhibitor (Supplementary

Fig. 4a, b). While DMOG stabilized hypoxia-inducible factor-1alpha (HIF-1 α), it did not affect the CABIN1 peptide and CNA interaction. Furthermore, we detected no hydroxyproline in the GST-tagged CABIN1 peptide or VIVIT peptide (Supplementary Fig. 4c). Next, we assessed *O*-linked glycosylation at the threonine residue of "PPTP." The *O*-linked glycosylation of GST-tagged peptides containing "PPTP" (CABIN1-L-1-2 and VIVIT PPTP) was not higher than that of the negative control or VIVIT peptide, indicating that no *O*-linked glycosylation occurred in the "PPTP" sequence (Supplementary Fig. 4c).

Previous phosphoproteomics experiments demonstrated the phosphorylation of CABIN1 threonines 2151 and 2154 during mitosis²⁹. To identify the modified residue in our model, we substituted each threonine with valine, which bears a methyl group instead of the hydroxyl group of threonine (Fig. 6a). Substituting threonine 6 (threonine 2151 of the full-length CABIN1) with valine (T6V) abolished the interaction between the CABIN1 peptide and CNA in the cellular and in vitro experiments. In contrast, substituting threonine 9 (threonine 2154 of the full-length CABIN1) with valine (T9V) abolished the interaction in the cellular experiment but not in vitro (Fig. 6b). Moreover, the T9V substitution restored the CABIN1-suppressed transcriptional activity of NFAT more efficiently than the T6V substitution (Fig. 6c). These results suggest that threonine 9 undergoes PTM, which increases the inhibitory effect on the CNA-NFAT pathway.

Indeed, we detected threonine 9 phosphorylation by Western blots using an antibody against phospho-MAPK substrates (PXpTP) in the Jurkat T cells expressing mCherry-tagged peptides (Fig. 6d). To directly detect the phosphorylated CABIN1 peptide in cells, we immunoprecipitated the HA-mCherry-tagged CABIN1 peptide with an anti-HA antibody from the Jurkat T cells expressing the protein. We analyzed the purified protein with LC-MS/MS and observed threonine 9 phosphorylation (Fig. 6e). Next, we synthesized a biotin-labeled VIVIT peptide, CABIN1 peptide, and phosphorylated CABIN1 peptide. A streptavidin pulldown assay with these peptides showed that CABIN1 phosphorylation dramatically increased the affinity for CNA (Fig. 6f). Finally, we quantitatively analyzed the binding affinity through surface plasma resonance (SPR). We observed that phosphorylation of the 9th threonine of the CABIN1 peptide increased the binding affinity by approximately threefold (Fig. 6g). Collectively, these results demonstrate that the CABIN1 peptide is a more efficient in vivo inhibitor than the VIVIT peptide because the phosphorylation of the threonine in "PPTP" enhances the binding affinity for CNA.

p38MAPK phosphorylates threonine 9 of the CABIN1 peptide PMA, an activator of PKC, induces CABIN1 hyperphosphorylation, but PKC does not directly phosphorylate CABIN1²⁰. Therefore, we investigated whether PMA causes the phosphorylation of the CABIN1 peptide—specifically the threonine of "PPTP"—and through which kinase. After PMA treatment, CABIN1 peptide phosphorylation increased two hours after treatment (Fig. 7a). To identify kinases that can directly phosphorylate the CABIN1 peptide, we performed an in vitro phosphorylation assay with

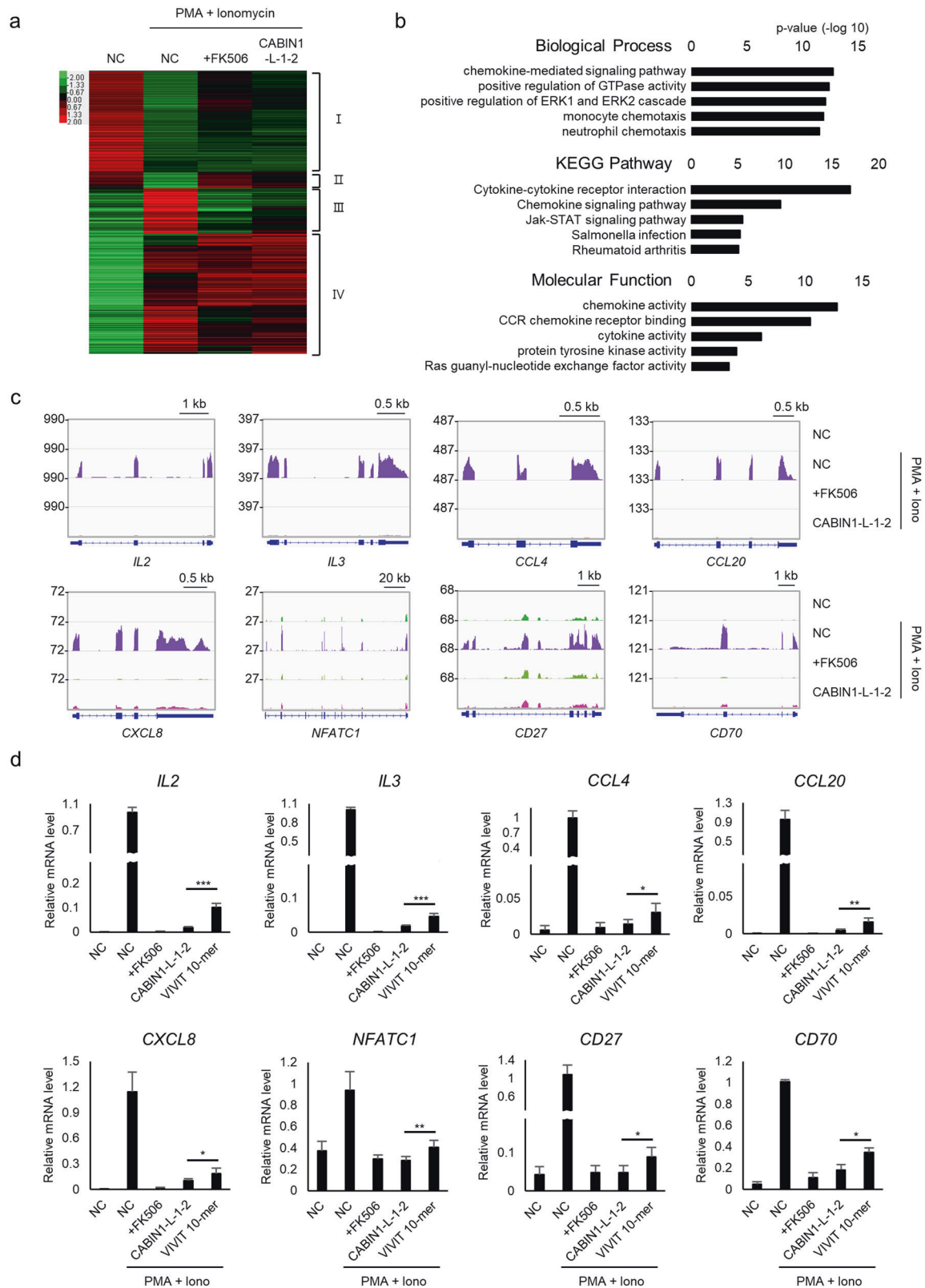


Fig. 3 The CABIN1 peptide inhibits T-cell activation. **a** Heatmap of altered genes affected by FK506 treatment or CABIN1 peptide expression upon T-cell activation. **b** Gene Ontology analysis of cluster III. **c** mRNA expression levels of genes included in cluster III. **d** qRT-PCR data of genes in **c**. The experiment was independently repeated at least three times, and the data are presented as the mean \pm standard deviation. Statistical differences were determined using two-tailed Student's *t*-test. * $p < 0.05$, ** $p < 0.01$, *** $p < 0.001$, NC negative control.

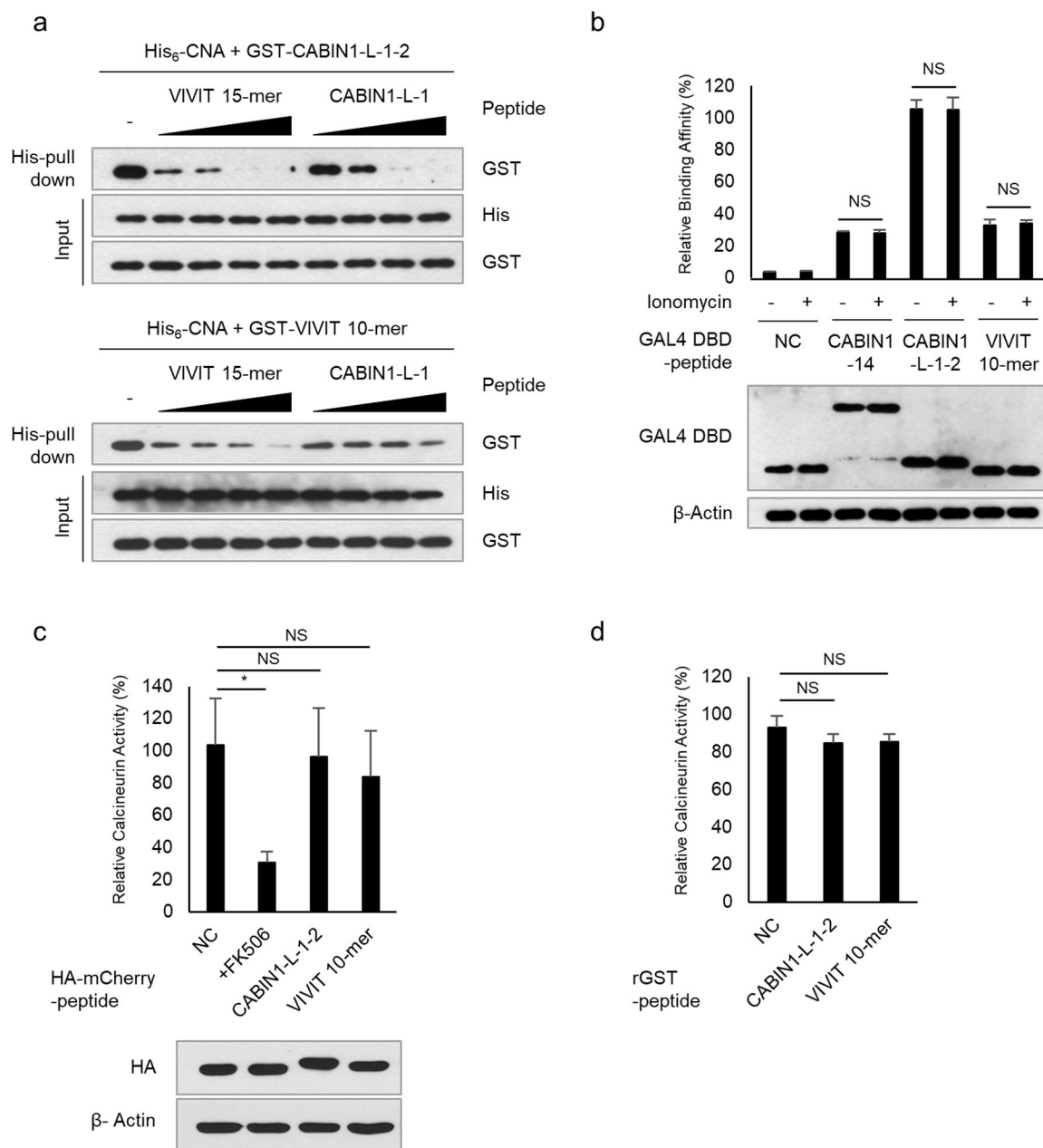


Fig. 4 The CABIN1 peptide does not affect calcineurin's phosphatase activity. **a** An in vitro peptide competition assay was conducted with the VIVIT 15-mer and CABIN1-L-1 peptides in a dose-dependent manner. The molar ratios of the GST-tagged peptide to the competing peptide ranged from 1:50 to 1:400. **b** A mammalian two-hybrid assay was performed using VP16 AD-CNA β_2 , and GAL4 DBD-peptides in the HEK293T cells with or without 1 μ M ionomycin treatment. pM empty vector was used as a negative control. **c** Calcineurin cellular activity assays were performed using Jurkat T cells expressing HA-mCherry-tagged peptides. Jurkat T cells expressing only HA-mCherry were used as a negative control, and cells treated with FK506 were used as a positive control. **d** In vitro calcineurin phosphatase activity assays using purified GST-tagged peptides. Purified GST was used as a negative control. All experiments were repeated three times, and the data are presented as the mean \pm standard deviation. Statistical differences were determined using one-way ANOVA. * $p < 0.05$, NS nonsignificant, NC negative control.

kinase candidates activated through PKC. We found that the MAPK family (ERK, JNK, and p38) and MKK4 directly phosphorylate the CABIN1 peptide (Fig. 7b). We focused on the MAPKs, considering that "PPTP" is a perfectly suited substrate motif for this family. ERK2, JNK1, and p38 α phosphorylated the purified recombinant GST-tagged peptides containing the "PPTP" sequence (CABIN1-L-1-2 and VIVIT PPTP) but not the GST-tagged VIVIT peptide (Fig. 7c). To investigate which kinases interact with CABIN1 in nature, we conducted an immunoprecipitation assay. This assay revealed that only p38 α was bound to CABIN1 at the cellular level (Fig. 7d). In addition, p38 α did not phosphorylate the

substituted PPTP sequences in vitro (Fig. 7e, f). We then confirmed that selective p38 inhibitors, such as EO 1428 or TAK 715, significantly reduced phosphorylation of the CABIN1 peptide, thereby decreasing its binding affinity for CNA (Fig. 7g, h). These results suggest that p38 α is an upstream kinase of the CABIN1 peptide in nature.

DISCUSSION

FK506 and cyclosporin A, respectively cooperating with FKBP12 or cyclophilin, spatially hinder the substrates' access to the active site

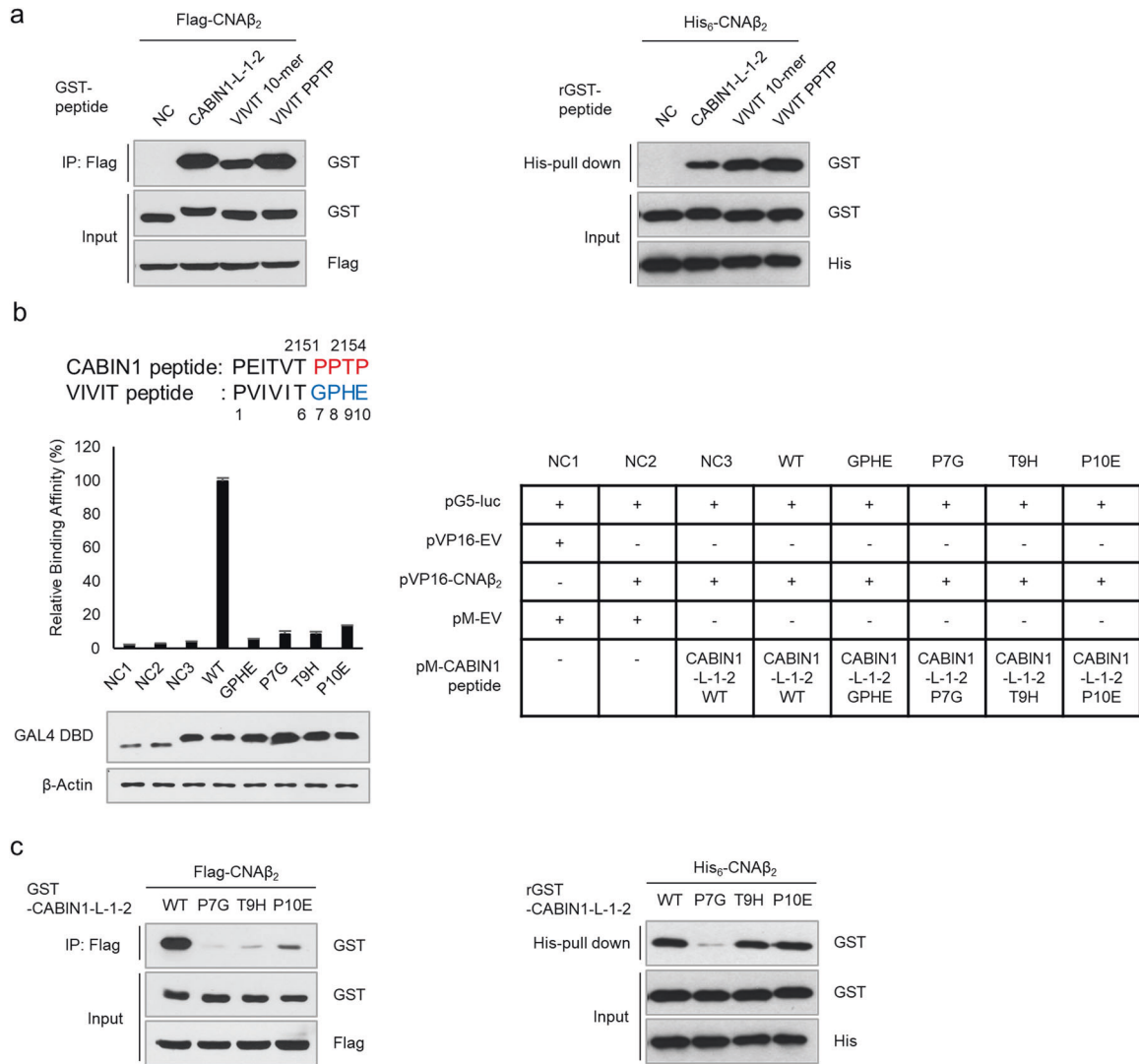


Fig. 5 The PPTP sequence is critical for the interaction with calcineurin at the cellular level. **a** Immunoprecipitation assay in HEK293T cells (left) and an in vitro His-pull-down assay (right) using the indicated tagged CNAβ₂ and peptides. **b** A mammalian two-hybrid assay was conducted using CNAβ₂ and substituted CABIN1 peptides to verify binding affinity ($n = 3$). HEK293T cells were transfected as described in the right panel. **c** Immunoprecipitation assay in HEK293T cells (left) and an in vitro His-pull-down assay using the indicated tagged CNAβ₂ and wild-type or substituted CABIN1 peptides (right). Values shown are the mean \pm standard deviation. NC negative control, WT wild-type.

of calcineurin, inhibiting its phosphatase activity^{30,31}. Long-term treatment with these drugs increases the expression of TGF-β and profibrogenic genes, such as collagen, fibronectin, and metalloproteinases³². Consequently, FK506 and cyclosporin A cause severe side effects, such as nephrotoxicity, fibrogenesis, neurotoxicity, and diabetes¹⁷.

To overcome these side effects, researchers have developed alternative inhibitors that specifically perturb the calcineurin-NFAT pathway. Among them, the VIVIT peptide showed better results than FK506 on allogeneic islet transplantation in mice without reducing insulin secretion³³. Furthermore, the VIVIT peptide showed potential as an alternative calcineurin inhibitor in treating cardiac hypertrophy and restenosis^{34,35}. This peptide also successfully suppressed the development of microbiota-dependent colorectal cancer by inhibiting the calcineurin-NFAT pathway in intestinal epithelial cells³⁶.

However, some characteristics of the VIVIT peptide (such as its stability and affinity) and peptide drug delivery systems require improvement before clinical use¹⁹. At present, a few studies have reported attempts to improve the VIVIT peptide. Most of them are related to delivery systems, such as conjugation with various cell-

penetrating peptides or the use of viral delivery systems^{33,36–38}. However, reports on VIVIT peptide binding affinity improvement are rare. In 2014, Qian, Dougherty et al. reported that the artificial peptidyl inhibitor ZIZIT-cisPro had a better binding affinity than the VIVIT peptide³⁹. However, since ZIZIT-cisPro does not exist in nature, it could trigger an immune response.

This study identified a key peptide sequence in the C-terminal fragment of CABIN1 that inhibited the calcineurin-NFAT pathway and clarified its mechanism. Based on this study, the CABIN1 peptide has two advantages over the VIVIT peptide. First, the CABIN1 peptide has a higher binding affinity for calcineurin than the VIVIT peptide. The CABIN1 peptide contains an N-terminal "PxlIT" motif and a "PPTP" sequence, which is different from the C-terminal "GPHEE" sequence of the VIVIT peptide. The C-terminal "PPTP" sequence endows this peptide with a higher affinity for CNA than the VIVIT peptide (Fig. 1d). This higher affinity for calcineurin allows the CABIN1 peptide to better disrupt the interaction between calcineurin and NFAT, ultimately blocking NFAT dephosphorylation and nuclear translocation more efficiently (Fig. 2b–e). Thus, the CABIN1 peptide successfully suppressed the expression of NFAT target genes upon T-cell

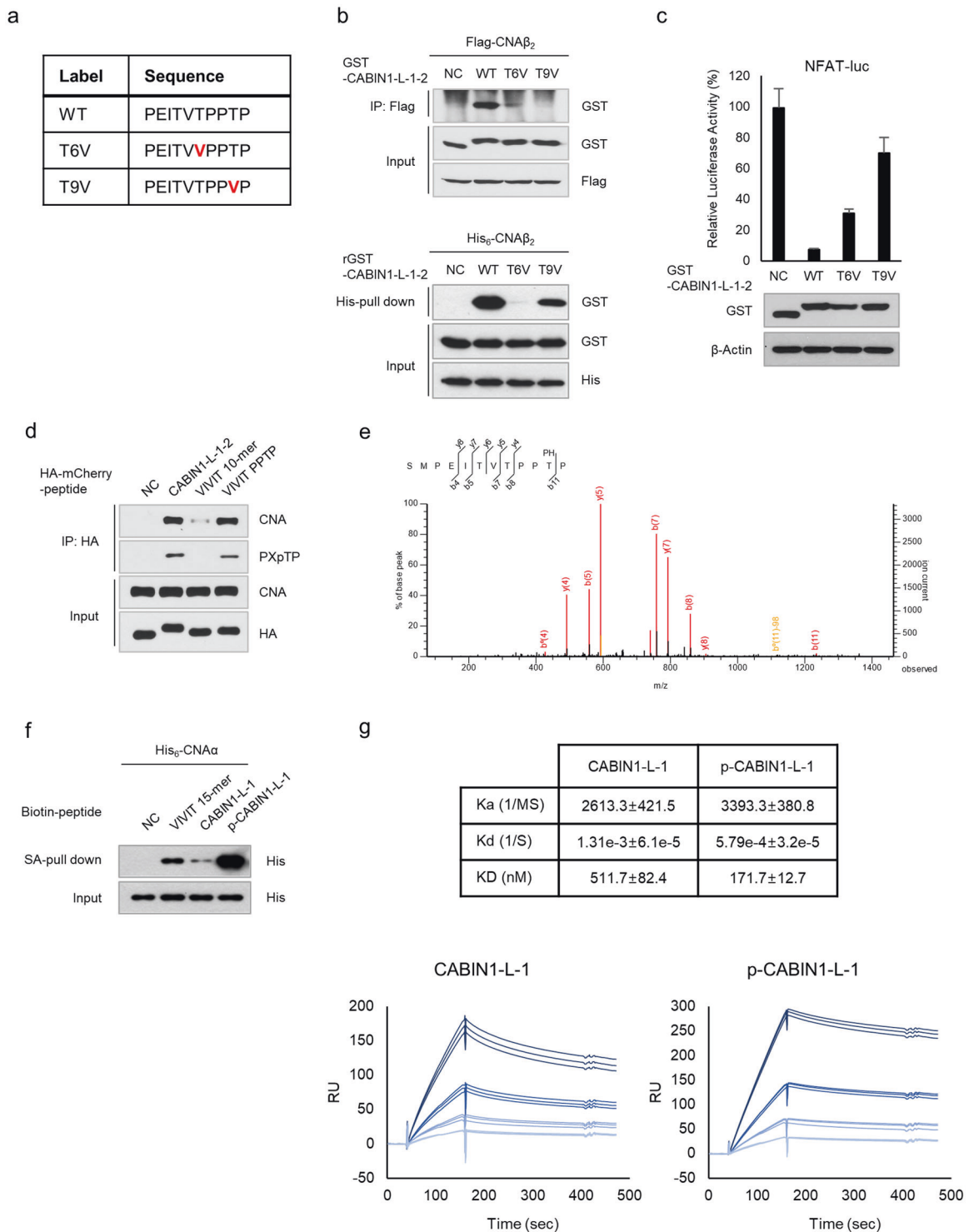


Fig. 6 Phosphorylation of CABIN1 T2154 is important for binding to calcineurin. **a** Sequence of threonine- to valine-substituted (TV) CABIN1 peptides. **b** Immunoprecipitation assay in HEK293T cells (top) and an in vitro His-pull-down assay (bottom) using the indicated tagged CNA β_2 and wild-type or TV CABIN1 peptides. **c** A luciferase reporter assay was performed to measure NFAT transcriptional activity in the Jurkat T cells expressing GST-tagged CABIN1 peptides under PMA and ionomycin treatment ($n = 3$). **d** Immunoprecipitation assay of the Jurkat T cells expressing HA-mCherry-tagged peptides using HA antibody. Peptide-bound CNA and phosphorylated threonine were detected by Western blotting. **e** Phosphorylation of the 9th threonine of the CABIN1 peptide (threonine 2154 of the full-length CABIN1) in Jurkat T cells was detected by LC-MS/MS. **f** An in vitro pull-down assay was performed using streptavidin-conjugated agarose beads. Biotinylated peptide-bound CNA was detected with His antibody. VEET peptide was used as a negative control. **g** CNA binding to biotinylated CABIN1 peptides with or without 9th threonine phosphorylation was measured by SPR. CNA concentrations ranged from 1.25, 2.5, 5, and 10 nM. The kinetics of interactions were calculated using the data of the CABIN1 peptide-captured cells minus the negative control peptide-captured cell. Values shown are the mean \pm standard deviation. RU response units, NC negative control.

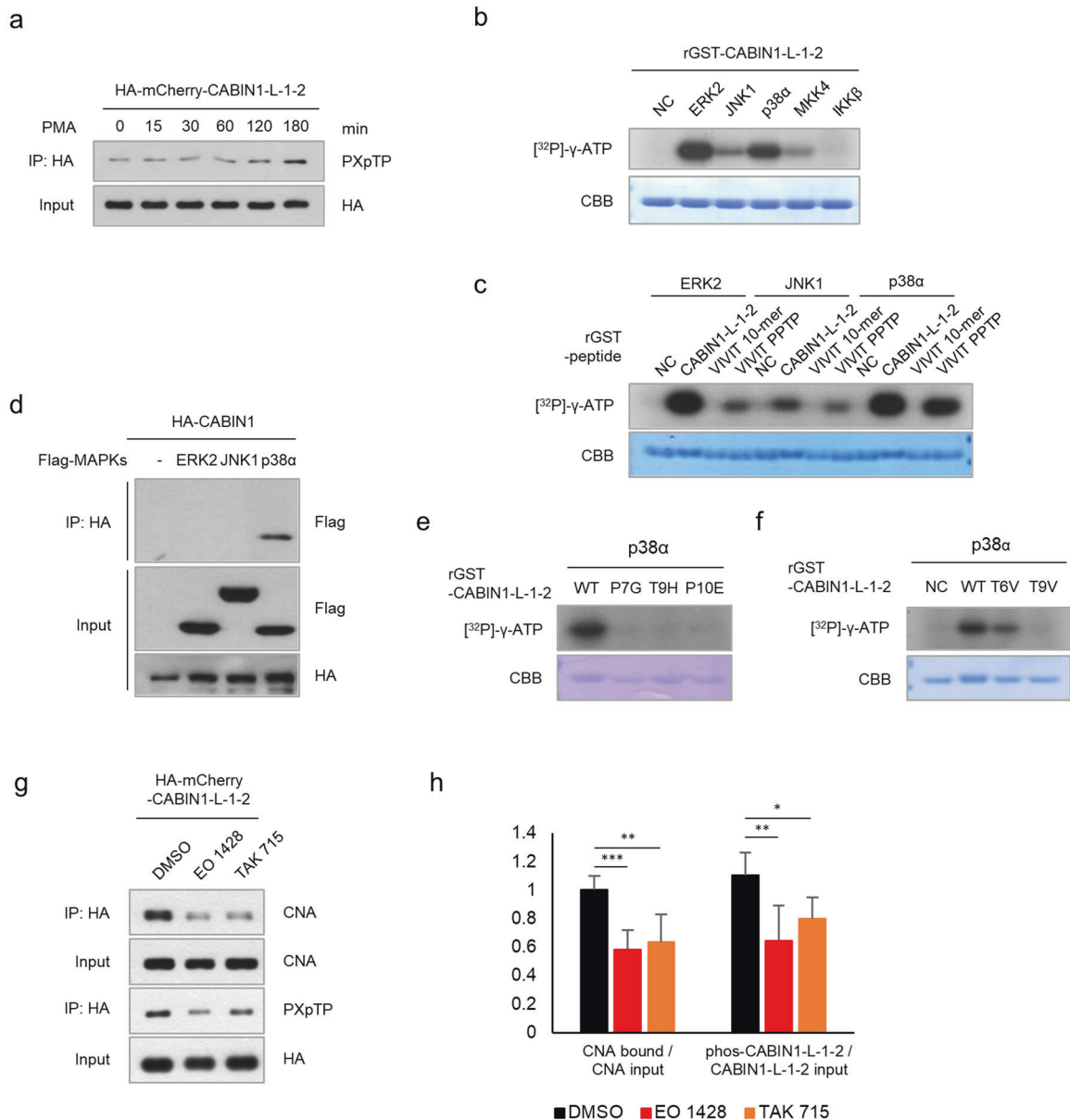


Fig. 7 p38MAPK phosphorylates the 9th threonine of the CABIN1 peptide. **a** Jurkat T cells expressing HA-mCherry-tagged CABIN1 peptide were treated with 40 nM PMA in a time-dependent manner. The phosphorylated threonine of the immunoprecipitated peptide with HA antibody was detected with [PXpTP] antibody. **b** In vitro kinase assays using purified GST-tagged CABIN1 peptide and PKC downstream kinases. **c** In vitro kinase assays using purified GST-tagged peptides and kinases included in the MAPK family. **d** Immunoprecipitation assays using Flag-MAPKs and HA-CABIN1 in HEK293T cells. **e, f** In vitro kinase assays using p38α and substituted CABIN1 peptides. **g** Jurkat T cells expressing HA-mCherry-tagged CABIN1 peptide were treated with 10 μM p38α inhibitors for 16 h. Immunoprecipitation was performed with HA antibody and detected by western blotting. **h** Phosphorylated threonine and peptide-bound CNA of **g** were measured using ImageJ, and the ratio of phosphorylation and calcineurin binding to the CABIN1 peptide was calculated ($n = 6$). Values shown are the mean \pm standard deviation. Statistical differences were determined using one-way ANOVA. * $p < 0.05$, ** $p < 0.01$, *** $p < 0.001$, CBB Coomassie Brilliant Blue, NC negative control.

activation much more efficiently than the VIVIT peptide (Fig. 3d). These results suggest that the CABIN1 peptide is a more efficient calcineurin inhibitor than the VIVIT peptide. However, the CABIN1 peptide only had a higher affinity at the cellular level, not in vitro (Fig. 5a), indicating that the CABIN1 peptide undergoes PTM which affects its binding affinity. Recent studies have suggested the importance of phosphorylated serine or threonine in calcineurin inhibitory peptides^{40,41}. However, no one has directly demonstrated their existence or role in nature. Here, we directly revealed the phosphorylation of the threonine of the "PPTP" sequence (T9) via LC-MS/MS and quantitatively demonstrated that

it increases the binding affinity to calcineurin (Fig. 6e, g). During Jurkat T-cell activation, the phosphorylation of nuclear NFAT and CABIN1 peptides by p38MAPK may cooperatively attenuate the immune response by inhibiting the reimportation of phosphorylated NFAT into the nucleus.

Next, the CABIN1 peptide is more stable than the full-length VIVIT peptide (15-mer) under physiological conditions. While comparing the VIVIT 15-mer with the VIVIT decamer, we found an interesting feature of the VIVIT peptide. The mCherry-tagged VIVIT peptide was dramatically less stable with C-terminal glutamate repeats (Supplementary Fig. 3b, c). The C-terminal glutamine repeat is the C-terminal

degron targeted by the CUL4/DCAF12 ubiquitin ligase complex⁴². Accordingly, when using the full-length VIVIT peptide, the tag type or location should be considered.

As an alternative calcineurin inhibitor, the CABIN1 peptide may exhibit advantages similar to those of the VIVIT peptide. These peptides compete to interact with CNA, implying that they bind to the same region and have the same mode of action (Fig. 4a). Since the CABIN1 peptide does not affect calcineurin's phosphatase activity (Fig. 4c, d), it probably does not perturb the dephosphorylation of calcineurin substrates other than NFAT. For instance, KSR2, another calcineurin substrate that interacts with calcineurin via the "LxVP" motif, is dephosphorylated by calcineurin in response to glucose stimulation. Dephosphorylated KSR2 induces ERK activation and insulin secretion³. Given that the CABIN1 and VIVIT peptides only carry the "PxIxIT" motif and not the "LxVP" motif, they probably do not interfere with the interaction between KSR2 and calcineurin. A previous report showed that the VIVIT peptide did not decrease insulin secretion in allogeneic islet transplantation in mice³³, supporting this assumption.

The present study found putative calcineurin target genes, such as *NINJ1* and *ZP4*, that are not regulated via the calcineurin-NFAT pathway. Upon T-cell activation, these genes were repressed by FK506 but unaffected by the CABIN1 and VIVIT peptides (Supplementary Fig. 5a, b). *NINJ1* encodes Ninjurin-1, a transmembrane adhesion molecule involved in axonal growth, inflammation, and cell death^{43,44}. Ninjurin-1 regulates inflammatory activation by modulating Toll-like receptor 4 signaling through direct binding to lipopolysaccharides in macrophages⁴⁵. *ZP4*, a component of the zona pellucida glycoproteins, promotes T-cell proliferation⁴⁶. Further studies should confirm whether these genes are associated with the side effects of FK506.

The interactive mechanism between calcineurin and its binding partners has not been fully elucidated. In addition to CABIN1, other calcineurin binding partners, such as AKAP79, RCAN1, and TRESK, carry a "PxIxIT" motif⁵. However, we found no reports investigating potential PTMs for their calcineurin binding regions. Our previous study showed that an internal fragment of CABIN1 that does not contain the "PxIxIT" or "LxVP" motif also inhibits calcineurin⁴⁷. Here, we revealed the detailed mechanism of CABIN1 as a calcineurin inhibitor and proved the superiority of the CABIN1 peptide over the VIVIT peptide for the first time. Modulation of the inhibitory effect through phosphorylation can be an advantage. Phosphorylation acts as a switch for the CABIN1 peptide, allowing it to target cells or tissues where p38 is highly activated. Given that the NFAT family contributes to the progression and metastasis of many cancers⁴⁸, the CABIN1 peptide could be used as an anticancer agent. Finally, our findings provide an alternative therapeutic strategy against various diseases related to the calcineurin-NFAT pathway.

REFERENCES

- Crabtree, G. R. & Clipstone, N. A. Signal transmission between the plasma membrane and nucleus of T-lymphocytes. *Annu. Rev. Biochem.* **63**, 1045–1083 (1994).
- Schulz, R. A. & Yutzey, K. E. Calcineurin signaling and NFAT activation in cardiovascular and skeletal muscle development. *Dev. Biol.* **266**, 1–16 (2004).
- Dougherty, M. K. et al. KSR2 is a calcineurin substrate that promotes ERK cascade activation in response to calcium signals. *Mol. Cell* **34**, 652–662 (2009).
- Baumgartel, K. & Mansuy, I. M. Neural functions of calcineurin in synaptic plasticity and memory. *Learn. Mem.* **19**, 375–384 (2012).
- Li, H., Rao, A. & Hogan, P. G. Interaction of calcineurin with substrates and targeting proteins. *Trends Cell Biol.* **21**, 91–103 (2011).
- Okamura, H. et al. Concerted dephosphorylation of the transcription factor NFAT1 induces a conformational switch that regulates transcriptional activity. *Mol. Cell* **6**, 539–550 (2000).
- Liu, J. O., Nacev, B. A., Xu, J. & Bhat, S. It takes two binding sites for calcineurin and NFAT to tango. *Mol. Cell* **33**, 676–678 (2009).

- Macian, F. NFAT proteins: key regulators of T-cell development and function. *Nat. Rev. Immunol.* **5**, 472–484 (2005).
- Schwartz, R. H. Models of T cell anergy: is there a common molecular mechanism? *J. Exp. Med.* **184**, 1–8 (1996).
- Macian, F. et al. Transcriptional mechanisms underlying lymphocyte tolerance. *Cell* **109**, 719–731 (2002).
- Loh, C., Carew, J. A., Kim, J., Hogan, P. G. & Rao, A. T-cell receptor stimulation elicits an early phase of activation and a later phase of deactivation of the transcription factor NFAT1. *Mol. Cell Biol.* **16**, 3945–3954 (1996).
- Su, B. et al. JNK is involved in signal integration during costimulation of T lymphocytes. *Cell* **77**, 727–736 (1994).
- Harhaj, E. W. & Sun, S. C. I κ B kinases serve as a target of CD28 signaling. *J. Biol. Chem.* **273**, 25185–25190 (1998).
- Rao, A., Luo, C. & Hogan, P. G. Transcription factors of the NFAT family: regulation and function. *Annu. Rev. Immunol.* **15**, 707–747 (1997).
- Tordai, A., Sarkadi, B., Gorog, G. & Gardos, G. Inhibition of the CD3-mediated calcium signal by protein kinase C activators in human T (Jurkat) lymphoblastoid cells. *Immunol. Lett.* **20**, 47–52 (1989).
- Gomez del Arco, P., Martinez-Martinez, S., Maldonado, J. L., Ortega-Perez, I. & Redondo, J. M. A role for the p38 MAP kinase pathway in the nuclear shuttling of NFATp. *J. Biol. Chem.* **275**, 13872–13878 (2000).
- Azzi, J. R., Sayegh, M. H. & Mallat, S. G. Calcineurin inhibitors: 40 years later, can't live without. *J. Immunol.* **191**, 5785–5791 (2013).
- Aramburu, J. et al. Affinity-driven peptide selection of an NFAT inhibitor more selective than cyclosporin A. *Science* **285**, 2129–2133 (1999).
- Yu, H., van Berkel, T. J. & Biessen, E. A. Therapeutic potential of VIVIT, a selective peptide inhibitor of nuclear factor of activated T cells, in cardiovascular disorders. *Cardiovasc. Drug Rev.* **25**, 175–187 (2007).
- Sun, L. et al. Cabin 1, a negative regulator for calcineurin signaling in T lymphocytes. *Immunity* **8**, 703–711 (1998).
- Kim, H. J. et al. Cyclin-dependent kinase 1 activity coordinates the chromatin associated state of Oct4 during cell cycle in embryonic stem cells. *Nucleic Acids Res.* **46**, 6544–6560 (2018).
- Lee, H. T. et al. Phosphorylation of OGFOD1 by cell cycle-dependent kinase 7/9 enhances the transcriptional activity of RNA polymerase II in breast cancer cells. *Cancers* **13**, 3418 (2021).
- Manders, E. M., Stap, J., Brakenhoff, G. J., van Driel, R. & Aten, J. A. Dynamics of three-dimensional replication patterns during the S-phase, analysed by double labelling of DNA and confocal microscopy. *J. Cell Sci.* **103**, 857–862 (1992).
- Bolte, S. & Cordelières, F. P. A guided tour into subcellular colocalization analysis in light microscopy. *J. Microsc.* **224**, 213–232 (2006).
- Dobin, A. et al. STAR: ultrafast universal RNA-seq aligner. *Bioinformatics* **29**, 15–21 (2013).
- de Hoon, M. J., Imoto, S., Nolan, J. & Miyano, S. Open source clustering software. *Bioinformatics* **20**, 1453–1454 (2004).
- Takeuchi, K., Roehrl, M. H., Sun, Z. Y. & Wagner, G. Structure of the calcineurin-NFAT complex: defining a T cell activation switch using solution NMR and crystal coordinates. *Structure* **15**, 587–597 (2007).
- Aramburu, J., Azzone, L., Rao, A. & Perussia, B. Activation and expression of the nuclear factors of activated T cells, NFATp and NFATc, in human natural killer cells: regulation upon CD16 ligand binding. *J. Exp. Med.* **182**, 801–810 (1995).
- Olsen, J. V. et al. Quantitative phosphoproteomics reveals widespread full phosphorylation site occupancy during mitosis. *Sci. Signal.* **3**, ra3 (2010).
- Griffith, J. P. et al. X-ray structure of calcineurin inhibited by the immunophilin-immunosuppressant FKBP12-FK506 complex. *Cell* **82**, 507–522 (1995).
- Jin, L. & Harrison, S. C. Crystal structure of human calcineurin complexed with cyclosporin A and human cyclophilin. *Proc. Natl Acad. Sci. USA* **99**, 13522–13526 (2002).
- Khanna, A., Plummer, M., Bromberek, C., Bresnahan, B. & Hariharan, S. Expression of TGF-beta and fibrogenic genes in transplant recipients with tacrolimus and cyclosporine nephrotoxicity. *Kidney Int.* **62**, 2257–2263 (2002).
- Noguchi, H. et al. A new cell-permeable peptide allows successful allogeneic islet transplantation in mice. *Nat. Med.* **10**, 305–309 (2004).
- Liu, Z., Zhang, C., Dronadula, N., Li, Q. & Rao, G. N. Blockade of nuclear factor of activated T cells activation signaling suppresses balloon injury-induced neointima formation in a rat carotid artery model. *J. Biol. Chem.* **280**, 14700–14708 (2005).
- Kuriyama, M. et al. A cell-permeable NFAT inhibitor peptide prevents pressure-overload cardiac hypertrophy. *Chem. Biol. Drug Des.* **67**, 238–243 (2006).
- Peuker, K. et al. Epithelial calcineurin controls microbiota-dependent intestinal tumor development. *Nat. Med.* **22**, 506–515 (2016).
- Choi, J. M., Sohn, J. H., Park, T. Y., Park, J. W. & Lee, S. K. Cell permeable NFAT inhibitory peptide Sim-2-VIVIT inhibits T-cell activation and alleviates allergic airway inflammation and hyper-responsiveness. *Immunol. Lett.* **143**, 170–176 (2012).

38. Lee, H. G., Kim, L. K. & Choi, J. M. NFAT-specific inhibition by dNP2-VIVITAmeliorates autoimmune encephalomyelitis by regulation of Th1 and Th17. *Mol. Ther. Methods Clin. Dev.* **16**, 32–41 (2020).
39. Qian, Z. et al. Structure-based optimization of a peptidyl inhibitor against calcineurin-nuclear factor of activated T cell (NFAT) interaction. *J. Med. Chem.* **57**, 7792–7797 (2014).
40. Nakamura, T. et al. Overexpression of C16orf74 is involved in aggressive pancreatic cancers. *Oncotarget* **8**, 50460–50475 (2017).
41. Nguyen, H. Q. et al. Quantitative mapping of protein-peptide affinity landscapes using spectrally encoded beads. *elife* **8**, e40499 (2019).
42. Koren, I. et al. The eukaryotic proteome is shaped by E3 ubiquitin ligases targeting C-terminal degrons. *Cell* **173**, 1622–1635 (2018).
43. Araki, T. & Milbrandt, J. Ninjurin, a novel adhesion molecule, is induced by nerve injury and promotes axonal growth. *Neuron* **17**, 353–361 (1996).
44. Kayagaki, N. et al. NIN1 mediates plasma membrane rupture during lytic cell death. *Nature* **591**, 131–136 (2021).
45. Shin, M. W. et al. Ninjurin1 regulates lipopolysaccharide-induced inflammation through direct binding. *Int. J. Oncol.* **48**, 821–828 (2016).
46. Choudhury, S., Ganguly, A., Chakrabarti, K., Sharma, R. K. & Gupta, S. K. DNA vaccine encoding chimeric protein encompassing epitopes of human ZP3 and ZP4: immunogenicity and characterization of antibodies. *J. Reprod. Immunol.* **79**, 137–147 (2009).
47. Jang, H., Cho, E. J. & Youn, H. D. A new calcineurin inhibition domain in Cabin1. *Biochem. Biophys. Res. Commun.* **359**, 129–135 (2007).
48. Mancini, M. & Toker, A. NFAT proteins: emerging roles in cancer progression. *Nat. Rev. Cancer* **9**, 810–820 (2009).

AUTHOR CONTRIBUTIONS

S.L. and H.-D.Y. provided the study concept and design. S.L., H.-T.L., Y.A.K., and I.-H.L. performed the experiments. C.-G.P. and K.C. analyzed the data. S.-J.K. and K.S. provided technical support. S.L. and H.-D.Y. prepared the manuscript.

FUNDING

This work was supported by National Research Foundation of Korea (NRF) grants funded by the Korean government (MIST) [2012R1A3A2048767 and 2021R1A2C3006559 to

H.-D.Y.], and supported by the Education and Research Encouragement Fund by Seoul National University Hospital.

COMPETING INTERESTS

The authors declare no competing interests.

ADDITIONAL INFORMATION

Supplementary information The online version contains supplementary material available at <https://doi.org/10.1038/s12276-022-00772-6>.

Correspondence and requests for materials should be addressed to Hong-Duk Youn.

Reprints and permission information is available at <http://www.nature.com/reprints>

Publisher's note Springer Nature remains neutral with regard to jurisdictional claims in published maps and institutional affiliations.



Open Access This article is licensed under a Creative Commons Attribution 4.0 International License, which permits use, sharing, adaptation, distribution and reproduction in any medium or format, as long as you give appropriate credit to the original author(s) and the source, provide a link to the Creative Commons license, and indicate if changes were made. The images or other third party material in this article are included in the article's Creative Commons license, unless indicated otherwise in a credit line to the material. If material is not included in the article's Creative Commons license and your intended use is not permitted by statutory regulation or exceeds the permitted use, you will need to obtain permission directly from the copyright holder. To view a copy of this license, visit <http://creativecommons.org/licenses/by/4.0/>.

© The Author(s) 2022